

A Dual Frequency (900 MHz and 58 GHz) Antenna for Communication Applications

Wolfgang Menzel, Maria Belen Espadas Lopez
Microwave Techniques, University of Ulm, D-89069 Ulm, Germany

Abstract

This contribution presents the combination of a microstrip patch antenna at 900 MHz and a folded reflector antenna at 58 GHz integrated in a common aperture. In this arrangement, the 58 GHz folded reflector antenna radiates through a grid integrated in the patch of the microstrip antenna. The properties of the 900 MHz antenna in this combination are equivalent to those of the patch antenna alone. The antenna at 58 GHz has beamwidths of 3.3° and 3.5° , a sidelobe level of better than -20 dB, and a gain of about 33 dB.

Zusammenfassung

Es wird die Integration von einer Mikrostreifenleitungs-Antenne bei 900 MHz und einer gefalteten Reflektorantenne für 58 GHz in einer gemeinsamen Apertur vorgestellt. Die 58 GHz Antenne strahlt dabei durch ein in die Mikrostreifenleitungsantenne integriertes Gitter. Die Eigenschaften der 900 MHz Antenne entsprechen denen einer Antenne ohne integrierte mm-Wellen-Antenne; die 58 GHz Antenne hat Keulenbreiten von $3,3^\circ$ und $3,5^\circ$, einen Nebenzipfelabstand von besser -20 dB und einen Gewinn von ca. 33 dB.

Introduction

Mobile communication systems work in the lower GHz range (0.9 GHz, 1.8 GHz), while tie lines to the base stations often are realized in the mm-wave range. This paper presents a possible combination of antennas for the 900 MHz and the 58 GHz range in a common aperture. This enables a very compact realization of small base stations, e.g. mounted at some building wall in a densely populated urban scenario. A reduced elevation beamwidth of the 900 MHz antenna can easily be achieved by placing further antenna elements (without integrated mm-wave antenna) below or above the antenna configuration described here.

Setup of the dual frequency antenna

The 900 MHz antenna is realized as a microstrip patch antenna over a low profile metal box, while the mm-wave antenna is integrated with this lower frequency antenna in the form of a folded reflector antenna [1] - [3]. The basic setup of this antenna configuration is shown in **Fig. 1**, together with a typical "ray" of the high gain 58 GHz antenna.

The 900 MHz patch antenna is placed on an inverted substrate ($\epsilon_r = 2.33$, $h = 1.58$ mm), acting at the same time as radom. The substrate is placed on top of a

resonator with air as dielectric (25 mm depth). The patch antenna is designed in a standard way using conventional CAD and MoM methods [4]. As the current on the patch mostly is concentrated at the edges, a circular grid structure (diameter 100 mm) easily can be incorporated into the patch metallization (**Fig. 2**), acting as polarizing grid for the 58 GHz antenna.

A thin reflector substrate ($\epsilon_r = 2.22$, $h = 0.254$ mm) with a special metallization pattern for the 58 GHz antenna (**Fig. 3**) is placed onto the ground plane of the antenna box of the patch antenna. The principal function of the folded reflector antenna is indicated in **Fig. 1**. The electric field of the feed radiation is polarized in such a way that it is reflected by the printed grid integrated in the low frequency patch. Following this, the wave is incident on the lower substrate (**Fig. 3**) with an array of printed dipoles. The dipoles are tilted by 45° with respect to the incident electric field. The field can be decomposed into components parallel to the axes of the dipoles. The geometrical dimensions of the dipoles are designed in such a way that, on the one hand, a phase difference of 180° occurs between the two components of the reflected wave, leading to a twisting of the polarization of the reflected wave by 90° (**Fig. 4**). On the other hand, an overall phase shift is achieved according to the focussing requirements. The original design of this antenna is done on the basis of periodic structures using spectral domain calculations [5].

In **Fig. 5**, a typical reflection phase behavior of a periodic arrangement of dipoles arranged on a quadratic grid is plotted as a function of element length and width. As can be recognized, phase mainly depends on dipole length, i.e. the dimension parallel to the electric field. Consequently, for the orthogonal polarization, the phase can be adjusted by the other dimension of the dipole nearly independently; the respective reflection phase angles for the orthogonal

polarization simply can be read from the data in Fig. 5 interchanging length and width of the metal elements. Thus, from this diagram, it is possible to select a large number of dipole dimensions having a phase shift of 180° between the reflected waves in the two polarizations, and, at the same time, different absolute reflection phase angles covering nearly 360° as required for the focussing function of the reflectarray.

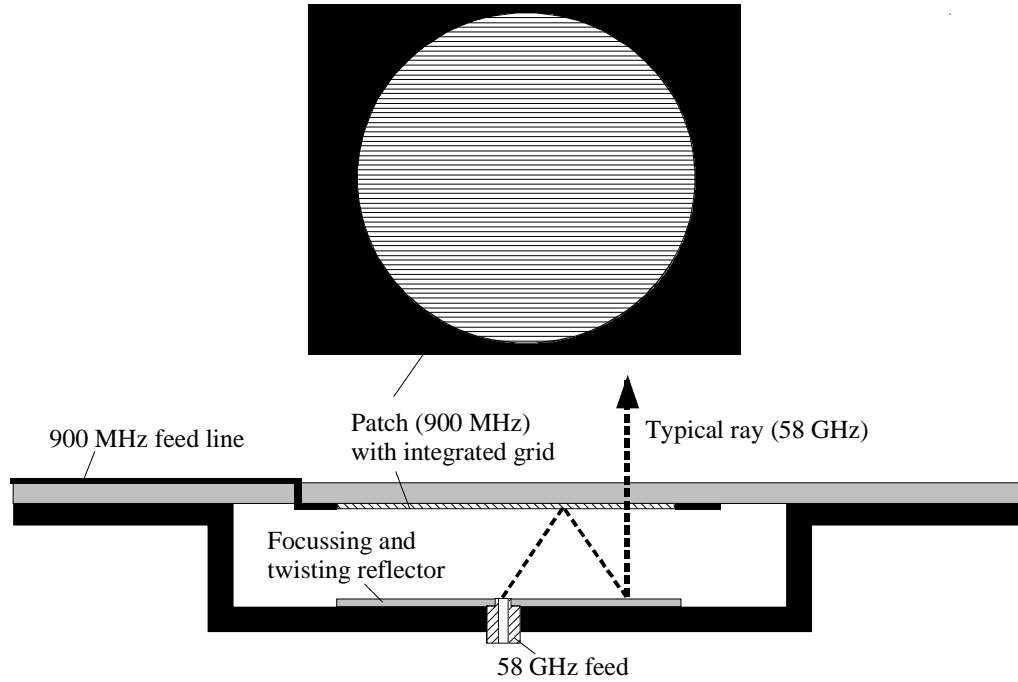


Fig. 1: Set-up of the dual frequency antenna.

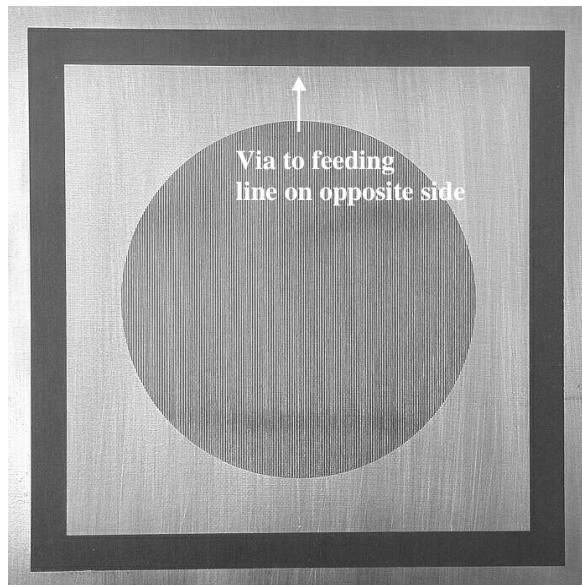


Fig. 2: Photograph of patch structure with integrated polarization grid (patch size 130 mm \times 130 mm).

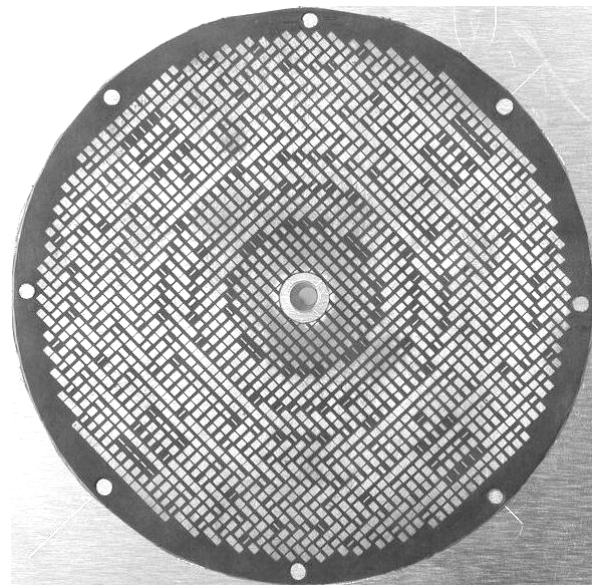


Fig. 3: Photograph of the 58 GHz focussing and reflecting array (reflector diameter 100 mm).

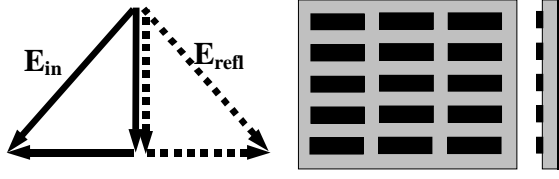


Fig. 4: Principle of polarization twisting by a printed periodic reflectarray.

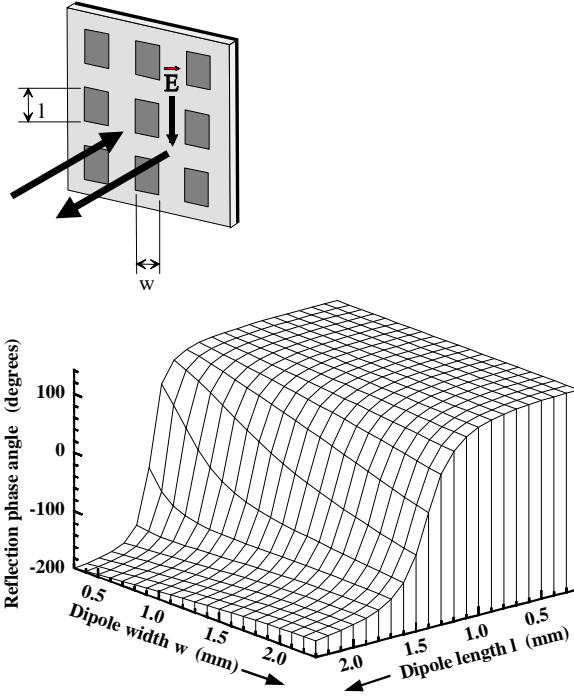


Fig. 5: Reflection phase angle of a plane wave reflected by a periodic array of printed dipoles. (Frequency 58 GHz, substrate thickness 0.254 mm, dielectric constant 2.22, dipole grid spacing 2.4 mm, normal incidence of the wave).

Results

The patch antenna without grid was originally designed and matched for 900 MHz and tested both for return loss and radiation diagram. In a second step, the grid as well as the reflector substrate and the 58 GHz feed were integrated, and the measurements were repeated.

Fig. 6 shows the return loss of the patch antenna without and with integrated grid. Except for the depth of the matching curve, only small differences can be stated. Bandwidth at -10 dB return loss is about 40 MHz (4.5 %) which certainly could be improved by a modified matching circuit. Hardly any influence

can be seen with respect to the radiation diagrams at 900 MHz (**Fig. 7**). As expected, the typical diagrams of a single patch result.

The 58 GHz diagrams are plotted in **Fig. 8**. Beamwidths are 3.3° and 3.5° in E- and H-plane, respectively. Sidelobe level in both planes is better than -20 dB. Gain has been measured in an antenna of comparable size but not integrated in such a patch arrangement and found to be around 33 dB. Compared to a gain of 33.7 dB calculated from the approximate formula $27000/(\Delta\Phi \times \Delta\Psi)$, where the beamwidths $\Delta\Phi$ and $\Delta\Psi$ are taken in degrees, losses are quite low.

Fig. 9 shows the measured E- and H-plane diagrams for an extended frequency range from 58 GHz to 62 GHz. Very similar results can be stated in this frequency range; an even wider bandwidth can be expected, although this was not tested. In this way, the folded reflector antenna covers not only the communication band around 58 GHz, but also the ISM band from 61 GHz to 61.5 GHz.

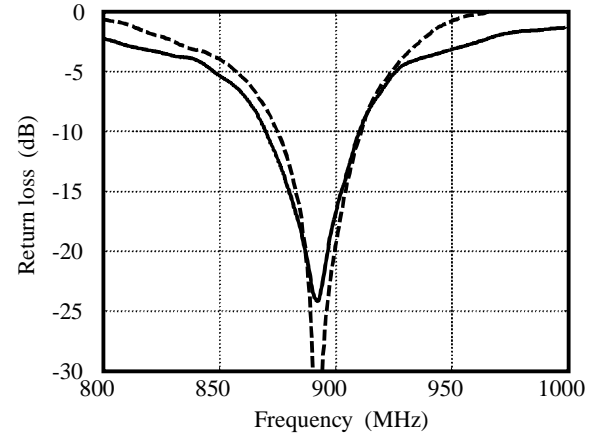


Fig. 6: Return loss of the 900 MHz patch antenna. Solid line: with integrated 58 GHz antenna; dashed line: 900 MHz patch antenna alone.

Conclusion

This presentation has demonstrated the design of a dual frequency antenna, covering both the mobile communication frequency band around 900 MHz, but also the communication band at 58 GHz together with the ISM band around 61 GHz. The 900 MHz antenna is based on a resonator backed microstrip patch antenna, while the mm-wave antenna consists of a folded reflector antenna with a polarizing grid integrated into a antenna patch, and a twisting and focussing planar reflector placed onto the bottom of the 900 MHz antenna box. Both antennas show excellent performance.

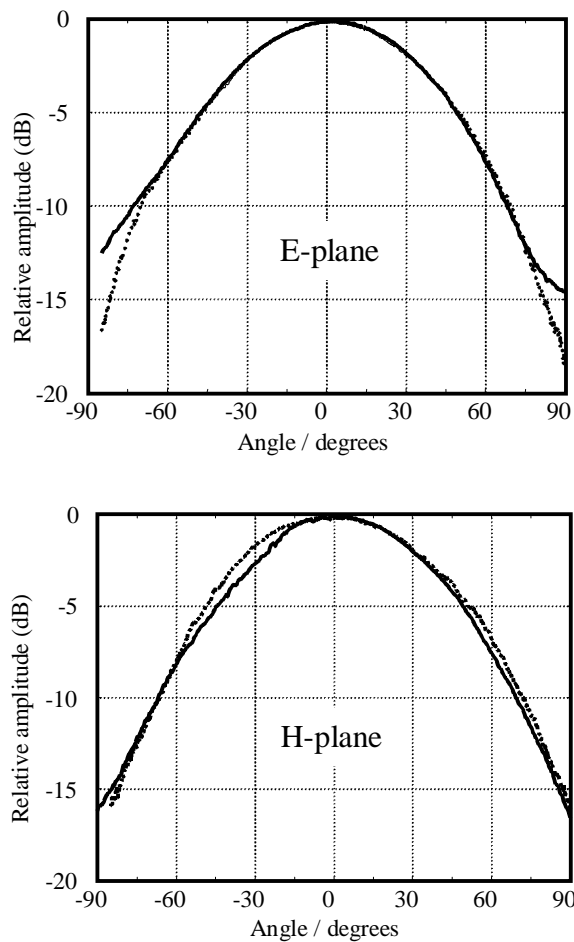


Fig. 7: E- and H-plane antenna radiation diagrams of the 900 MHz antenna. Solid line: with integrated 58 GHz antenna; dashed line: 900 MHz patch antenna alone.

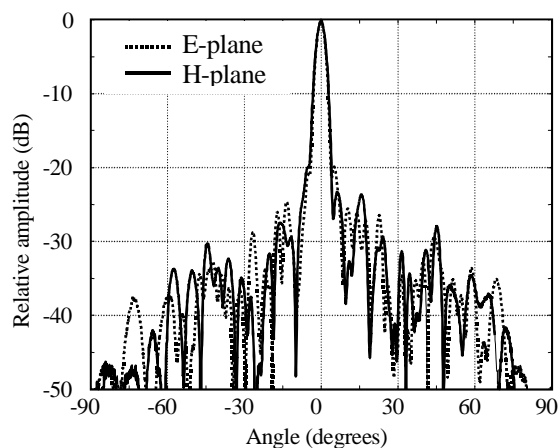


Fig. 8: E- and H-plane radiation diagrams of the integrated folded reflector antenna at 58 GHz.

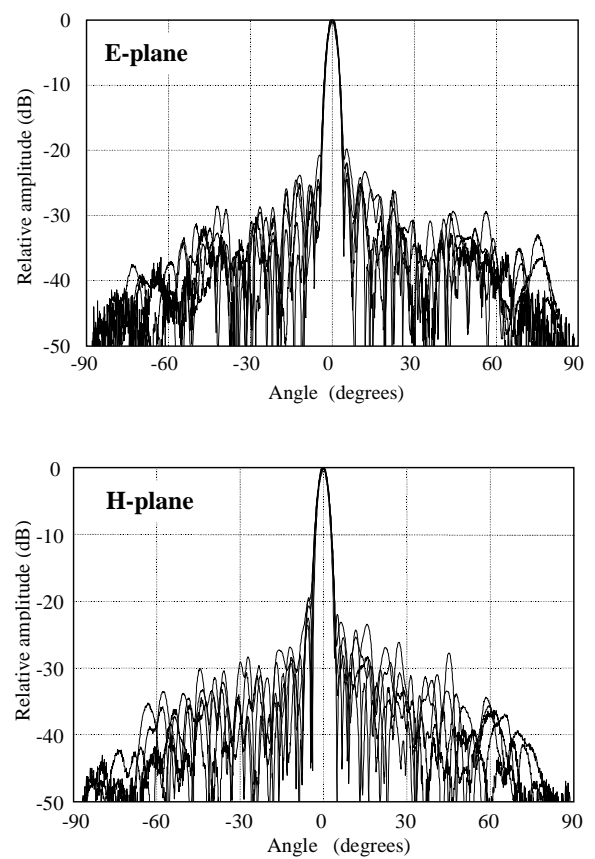


Fig. 9: E- and H-plane radiation diagrams of the integrated folded reflector antenna at 58 GHz, 59 GHz, 60 GHz, 61 GHz, and 62 GHz.

References

- [1] Pilz, D., Menzel, W.: Folded reflectarray antenna. *Electron. Lett.*, Vol. 34, No. 9, April 1998, pp. 832 – 833.
- [2] Menzel, W., Pilz, D.: Printed quasi-optical mm-wave antennas. *Millenium Conf. on Antennas and Propagation AP2000*, Davos, Switzerland, 2000, Session 3A2-1 (Paper 0023).
- [3] Pilz, D., Menzel, W.: Printed Millimeter-Wave Reflectarrays. *Annales de Telecommunications*, Vol. 56 (2001), No. 1-2, pp. 2-11.
- [4] Momentum in HP-ADS.
- [5] Itoh, T. (editor), *Numerical Techniques For Microwave And Millimeter-Wave Passive Structures*. John Wiley & Sons, 1989